

## Final scientific report

Project PN-III-P1-1.1-PD-2019-1303 (contract PD 211 / 2020)

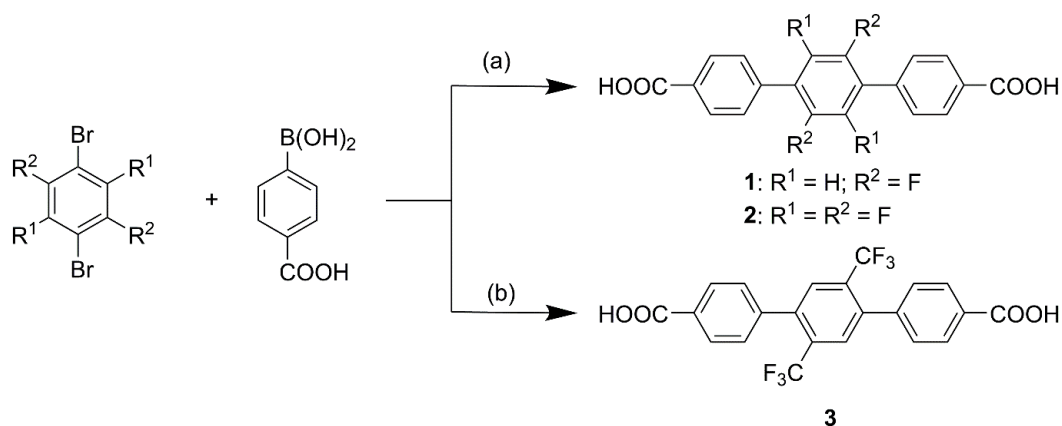
Project name: Metal-organic frameworks based on fluorinated terphenilic ligands for gas storage and separation

Acronym: FluoroMOF

The devised and accomplished project objectives are:

1. The synthesis of the fluorinated aromatic carboxylic acids and their structural characterization (elemental analysis, NMR, IR).
2. The synthesis of porous coordination polymers with the new ligands and transitional metal salts.
3. Evaluation of the metal-organic frameworks thermal and water stability, surface area and pore volume and preferential gas adsorption/separation ability.
4. Scientific results dissemination through the publication of at least two scientific papers in Web of Science indexed journal, at least one of which will be open access alongside the participation of at least two national or international scientific events with either oral or poster presentations.
5. Performing a research stay abroad at the Institute for Inorganic Chemistry and Structural Chemistry Heinrich-Heine-University Düsseldorf, Germany, under the supervision of the Mentor Prof. Dr. Christoph Janiak.

In accordance with the project plan, in the first stage the synthesis of the three proposed ligands has been accomplished (**Objective 1**). The compounds 2',5'-difluoro-[1,1':4',1''-terphenil]-4,4''-dicarboxylic acid H<sub>2</sub>F<sub>2</sub> and 2',3',5',6'-tetrafluoro-[1,1':4',1''-terphenil]-4,4''-dicarboxylic acid H<sub>2</sub>F<sub>4</sub>, have been synthesized in a single step through a Suzuki-Miyaura coupling reaction (Scheme 1a). For the preparation of the third ligand 2',5'-bis(trifluoromethyl)-[1,1':4',1''-terphenil]-4,4''-dicarboxylic acid H<sub>2</sub>CF<sub>3</sub>, 2 steps were needed-one for bromination of the substrate 1,4-bis(trifluoromethyl)benzene followed by the same Suzuki-Miyaura coupling reaction.



**Scheme 1.** Synthetic approach towards the three reported ligands. Reaction conditions: (a)  $\text{Pd}(\text{PPh}_3)_4$ ,  $\text{K}_2\text{CO}_3$ , THF:water (5:1 v/v), reflux, 72 h; (b)  $\text{Pd}(\text{PPh}_3)_4$ ,  $\text{K}_2\text{CO}_3$ , dioxane:ethanol:water (4:1:1 v/v/v), reflux, 72 h.

The encountered difficulties regarding the precursors and final compounds solubility have been overcome through the judicious identification of the adequate solvent mixtures: THF:water (5:1 v/v) for the synthesis of compounds **1** and **2**, or dioxane:ethanol:water (4:1:1 v/v/v) for compound **3**.

The Suzuki-Miyaura coupling reaction used for the synthesis of the three aromatic dicarboxylic acids was achieved by dissolving the corresponding brominated substrate (1,4-dibromo-2,5-difluorobenzene for **1**, 1,4-dibromo-2,3,5,6-tetrafluorobenzene for **2** and 1,4-dibromo-2,5-bis(trifluoromethyl)benzene for **3**) in the solvent mixture (previously degassed) alongside 4-carboxyphenylboronic acid and potassium carbonate. After ensuring an inert atmosphere by argon sparging, the catalyst Tetrakis(triphenylphosphine)palladium(0)  $\text{Pd}(\text{PPh}_3)_4$  was added. The reaction mixtures were refluxed for 72 h. After the reactions were finalized, the pH of the reaction mixtures was brought to 1-2 units using 36% hydrochloric acid under vigorous stirring and the resulting precipitate were collected by filtration, washed with water and ethanol (for compounds **1** and **2**) until neutral pH. The crude products were recrystallized from DMF and subjected to hot filtration in order to remove the palladium catalyst traces. The reaction yields for all three coupling reactions were greater than 70%.

The ligands structure and purity were confirmed by  $^1\text{H}$ ,  $^{13}\text{C}$  and  $^{19}\text{F}$  NMR spectroscopy (Figure 1-3), FT-IR spectroscopy and elemental analysis (**Objective 1**).

Elemental analysis and FT-IR bands:

(i) 2',5'-difluoro-[1,1':4',1''-terphenil]-4,4''-dicarboxylic acid **1**: Anal. Calculated for  $\text{C}_{20}\text{H}_{12}\text{F}_2\text{O}_4$ : C, 67.81; H, 3.41. Found: C, 68.13; H, 3.53.

FT-IR ( $\nu$ ,  $\text{cm}^{-1}$ ): 2669 (vw), 2545 (vw), 1934 (vw), 1689 (vs), 1608 (s), 1569 (w), 1523 (m), 1485 (s), 1427 (s), 1390 (s), 1321 (s), 1292 (s), 1166 (m), 1110 (m), 1037 (vw), 1010 (w), 923 (m), 893 (m), 854 (s), 815 (w), 767 (s), 702 (s), 667 (w), 549 (s), 505 (m), 466 (m).

(ii) 2',3',5',6'-tetrafluoro-[1,1':4',1''-terphenil]-4,4''-dicarboxylic acid **2**; Anal. Calculated for C<sub>28</sub>H<sub>28</sub>F<sub>4</sub>N<sub>2</sub>O<sub>6</sub> : C, 59.58; H, 4.99, N, 4.96. Found: C, 59.99; H, 4.43, N, 5.11.

FT-IR (v, cm<sup>-1</sup>): 2673 (w), 2547 (w), 1695 (vs), 1610 (m), 1566 (w), 1477 (s), 1423 (s), 1402 (s), 1296 (s), 1188 (w), 1114 (w), 1018 (w), 981 (s), 910 (m), 856 (m), 837 (w), 788 (m), 767 (m), 748 (vw), 700 (m), 547 (m), 487 (w).

(iii) 2',5'- bis(trifluoromethyl)-[1,1': 4',1''-terphenil]-4,4''-dicarboxylic acid **3**: Anal. Calculated for C<sub>28</sub>H<sub>26</sub>F<sub>6</sub>N<sub>2</sub>O<sub>6</sub>: C, 56.01; H, 4.36, N, 4.66. Found: C, 56.41; H, 4.22, N, 4.81.

FT-IR (v, cm<sup>-1</sup>): 2671 (vw), 2544 (vw), 1697 (vs), 1608 (m), 1566 (w), 1523 (w), 1498 (w), 1417 (s), 1286 (s), 1247 (s), 1136 (vs), 1087 (s), 1029 (m), 929 (w), 904 (m), 858 (m), 808 (w), 777 (m), 757 (w), 705 (s), 659 (w), 621 (w), 588 (w), 551 (s), 536 (m), 482 (w).

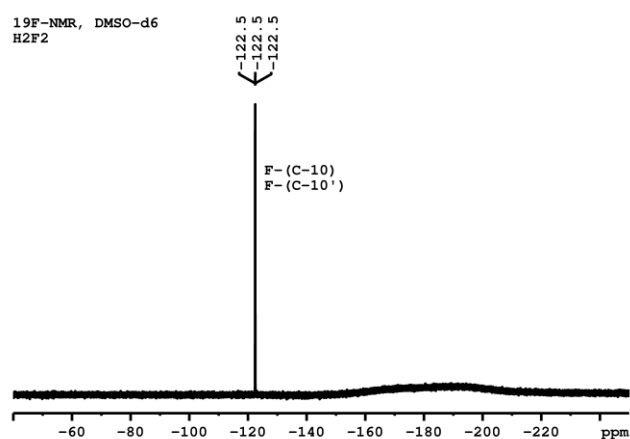
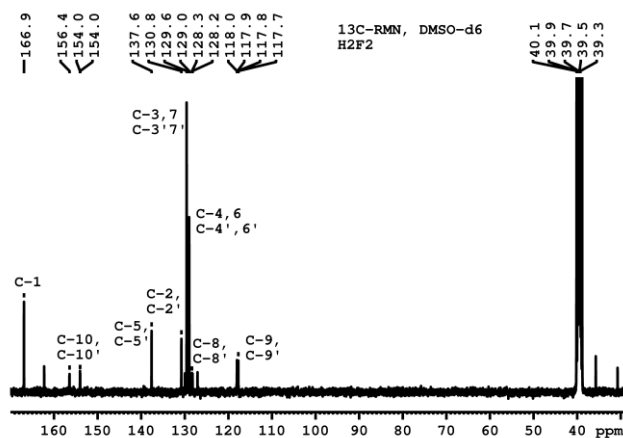
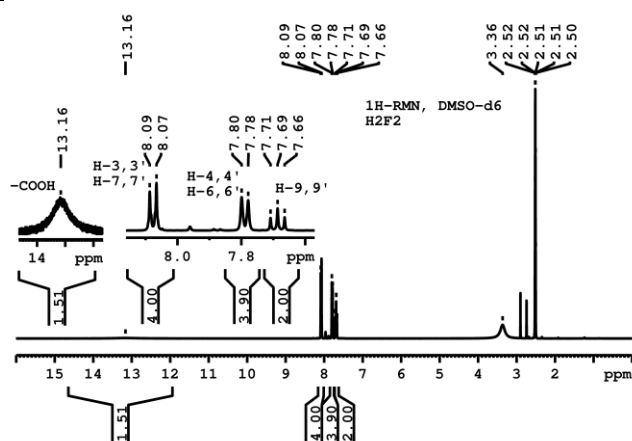
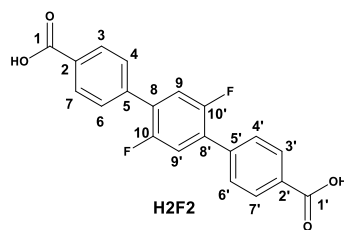


**Figure 1.** Annotated structure and <sup>1</sup>H, <sup>13</sup>C and <sup>19</sup>F NMR spectra of 2',5'-difluoro-[1,1':4',1''-terphenil]-4,4''-dicarboxylic acid **1**.

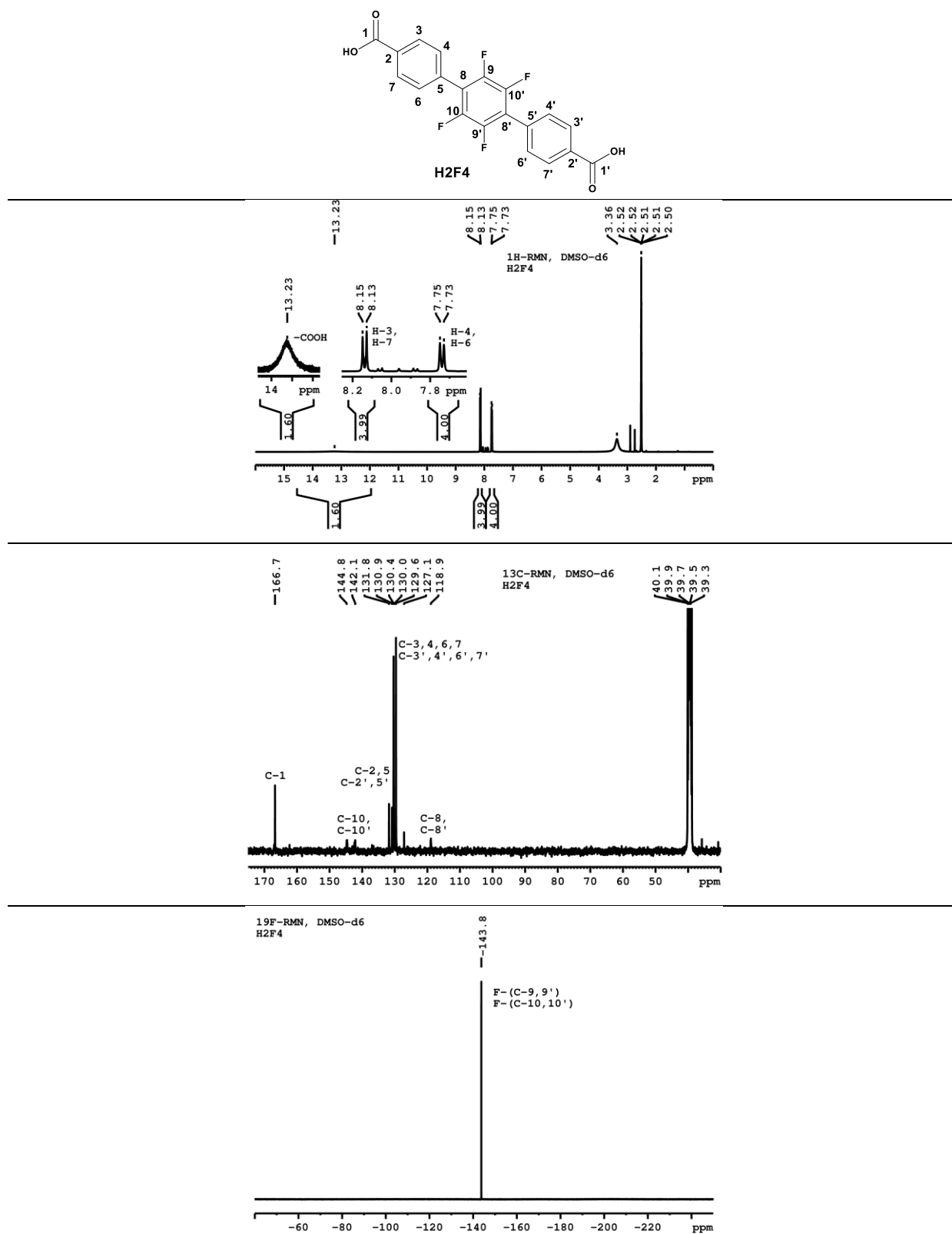


**Figure 2.** Annotated structure and <sup>1</sup>H, <sup>13</sup>C and <sup>19</sup>F NMR spectra of 2',3',5',6'-tetrafluoro-[1,1':4',1''-terphenil]-4,4''-dicarboxylic acid **2**.

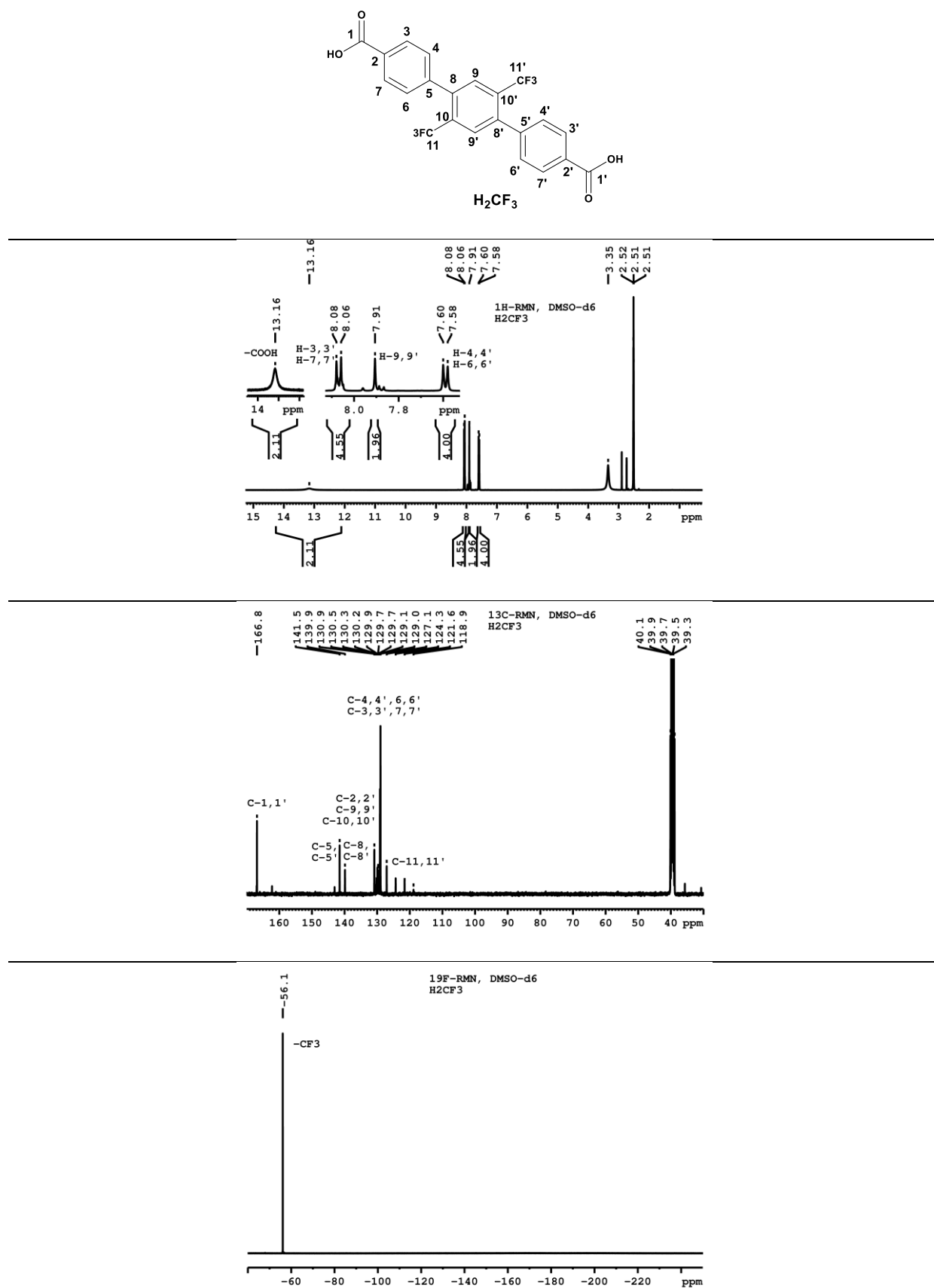


**Figure 3.** Annotated structure and  $^1\text{H}$ ,  $^{13}\text{C}$  and  $^{19}\text{F}$  NMR of 2',5'- bis(trifluoromethyl)-[1,1':4',1''-terphenil]-4,4''-dicarboxylic acid **3**.

Recrystallization from DMF afforded the isolation of 2',5'-difluoro-[1,1':4',1''-terphenil]-4,4''-dicarboxylic acid **1** and 2',5'- bis(trifluoromethyl)-[1,1':4',1''-terphenil]-4,4''-dicarboxylic acid **3** as crystals, while 2',3',5',6'-tetrafluoro-[1,1':4',1''-terphenil]-4,4''-dicarboxylic acid **2** was obtained in this form after recrystallization from dimethylacetamide. The crystals were subjected to single crystal X-ray diffraction which further confirmed the structure and geometry of the ligands (Figure 4).

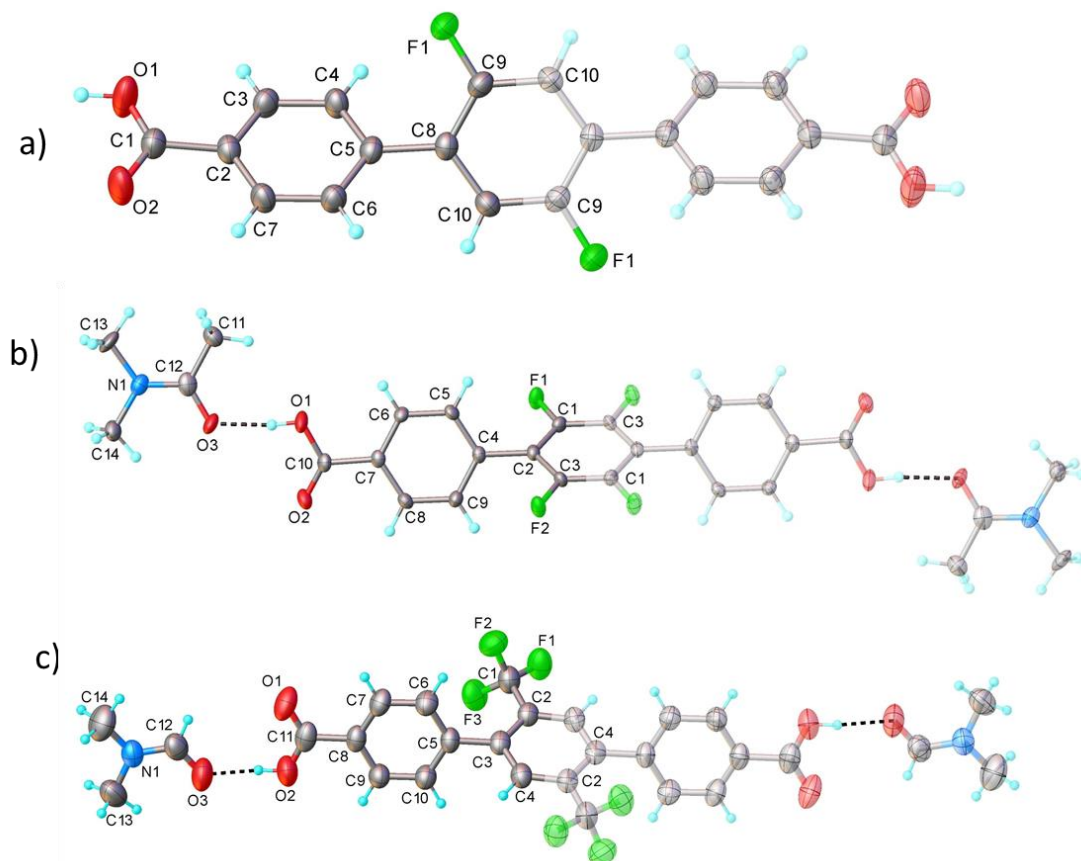


**Figure 4.** X-ray molecular structure with atom labeling and thermal ellipsoids at 50% probability for **1** (a), **2** (b) and **3** (c). Symmetry generated fragments are shown with faded colors. Only the major position occupied by disordered fluorine atoms in the molecule of compound **1** is shown.

The identification of the X-ray molecular structure of all three aromatic dicarboxylic acids allowed the calculation of the Hirshfeld surface analysis, which identifies the supramolecular packing and atom proximities in the crystalline solid. In addition, starting with from the X-ray molecular structure, a molecular modeling study was carried out. The results revealed that the presence of the substituents (either fluorine atoms or trifluoromethyl groups) in the central phenyl ring in ortho positions relative to the terminal phenyl rings induces a twisting effect in all target compounds. The twisting effect can be due of the sterical repulsion between fluorine atoms in the central phenyl ring and spatially neighboring hydrogen atoms in the terminal phenyl rings because the distances between these atoms in a theoretical fully planar structure of the terphenyl core are shorter than the sum of van der Waals radii. Based on the quantum chemical calculations the chemical

reactivity, chemical stability, and active regions in chemical reactions of the target compounds were estimated from ESP representations and frontier HOMO-LUMO gap. Moreover, the theoretical results predicted by ESP representation show the presence of the partially neutral charges on the fluorine atoms which explained the twisting effect.

### **The synthesis of coordination polymers with the three fluorinated aromatic ligands and transitional metal salts (Objective 2).**

Initially, preliminary reactions were screened in order to facilitate the isolation of UiO-68 type MOFs in crystal form. DMF was used as the reaction solvent and zirconium chloride as the metal salt. The reaction temperature, acid modulator type and quantity were varied. Before heating the reaction vials to the desired temperature, the reaction mixtures were homogenized in an ultrasound bath for 15 minutes. Notable results were obtained from solvothermal reactions (120 °C, 72 h) using acetic (exp 13F2) or trifluoroacetic (exp 15F2) as acidic reaction modulators. The identified reaction conditions afforded the isolation of a coordination polymer composed of the deprotonated ligand 2',5'-difluoro-[1,1':4',1''-terphenil]-4,4''-dicarboxylic acid H<sub>2</sub>F<sub>2</sub> and zirconium (Zr-F<sub>2</sub>) as crystals which lead to the identification of the structure through single crystal X-Ray diffraction (Figure 5).

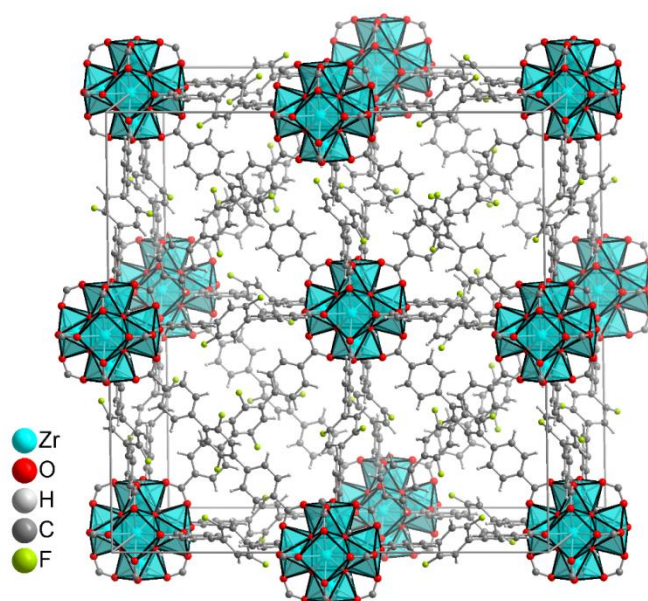


**Figure 5.** Graphical representations of the 3D structure obtained by single crystal X-ray diffraction of the MOF composed of ligand 2',5'-difluoro-[1,1':4',1''-terphenil]-4,4''-dicarboxylic acid H<sub>2</sub>F<sub>2</sub> and zirconium (Zr-F<sub>2</sub>).

With the help of powder X-ray diffraction, the phase purity of the two samples in comparison with the calculated diffractogram (from the single crystal structure) was confirmed (Figure 6). In addition, the iso-structurality of the MOFs prepared using the two identified reaction protocols was confirmed using the same characterization technique.



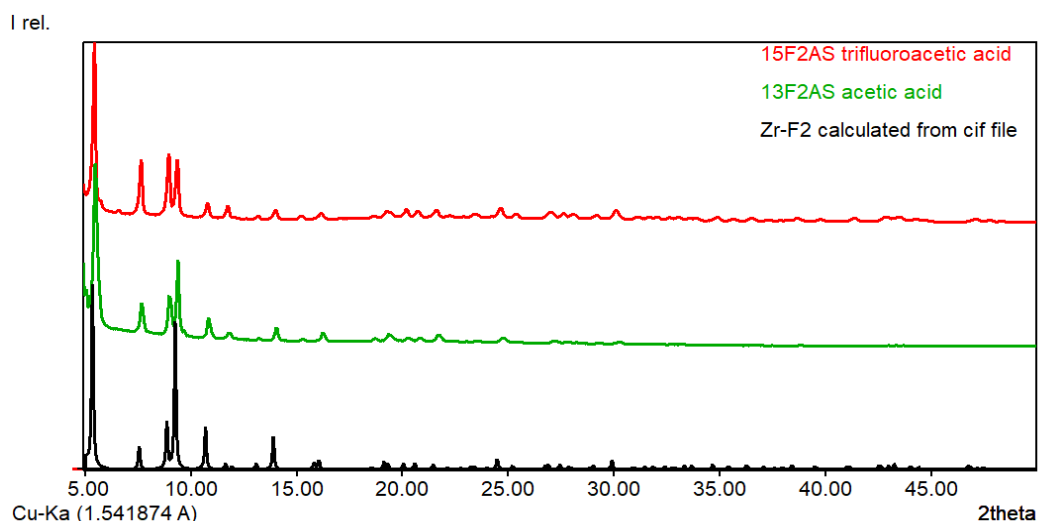


**Figure 6.** The diffractograms of the Zr-F2 MOFs prepared in the presence of acetic acid (green) and trifluoroacetic acid (red) in comparison with the calculated diffractogram using the single crystal structure (black).

The use of a higher reaction temperature (125 and 130 °C) reduces the reaction time to 48 h but the phase purity decreases due to the formation of an amorphous phase. The experiments were repeated in triplicate using the initial conditions to confirm the reproducibility of the reaction protocols. The results showed that the optimal protocol was the one where acetic acid was the modulator. In addition, the same reaction was up-scaled (x2 and x4) in order to obtain the Zr-F2 MOF in an adequate quantity necessary for the characterization and properties evaluation of the coordination polymer. With the help of pXRD, the reaction protocol was validated by means of reproducibility and up-scalability (Figure 7). The purification of the MOF was accomplished by repeated washing with DMF, centrifugation and removal of the supernatant, followed by a rapid washing with methanol and drying in an oven at 80 °C. The reaction yield in all the repeated experiments at the same scale or up-scaled was between 60-70%.

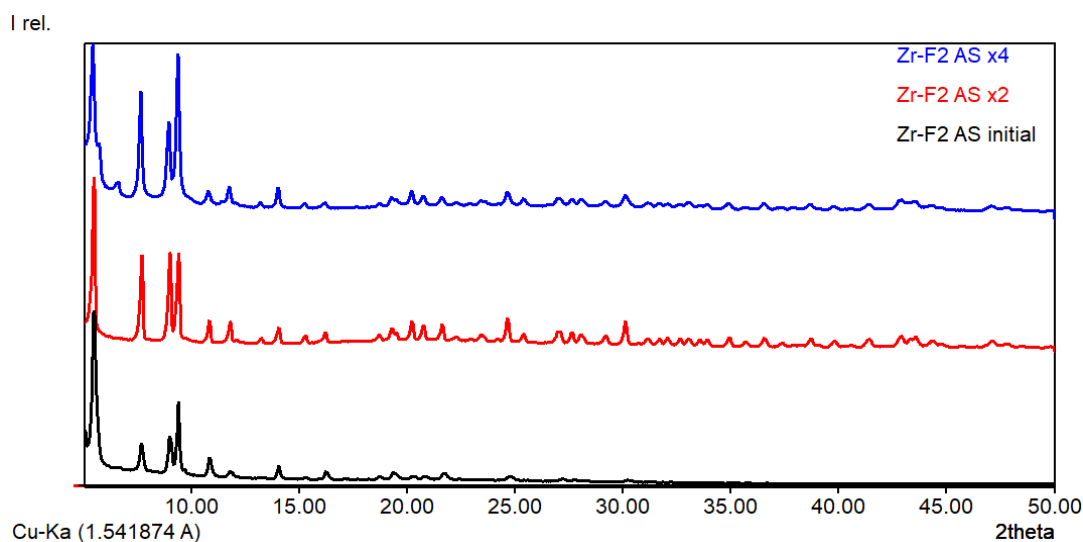


**Figure 7.** Zr-F2 diffractograms: the initial experiment (black), up-scaled 2x (red) and 4x (blue), synthesized in the presence of acetic acid.

Evaluation of the Zr-F2 thermal stability (Figure 8) indicated that the 3D network retains a large quantity of solvents due to its porous nature, as evidenced by a 25 % mass loss in the 34-400 °C interval, while the actual decomposition begins after 500 °C.

(Figure 8).

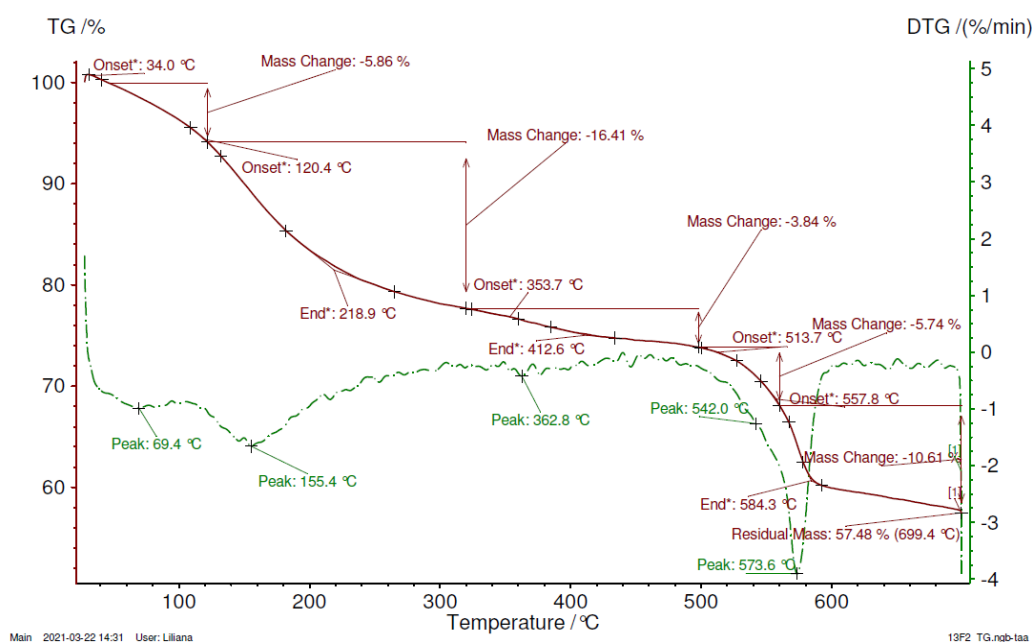


**Figure 8.** Zr-F2 MOF TGA-DTG curve.

After the thermal decomposition threshold was established, the thermal activation of the network was made at 150 °C, under vacuum ( $10^{-2}$  mbar). After the activation, the nitrogen adsorption and desorption isotherms were recorded (Figure 9).- **Objective 3**

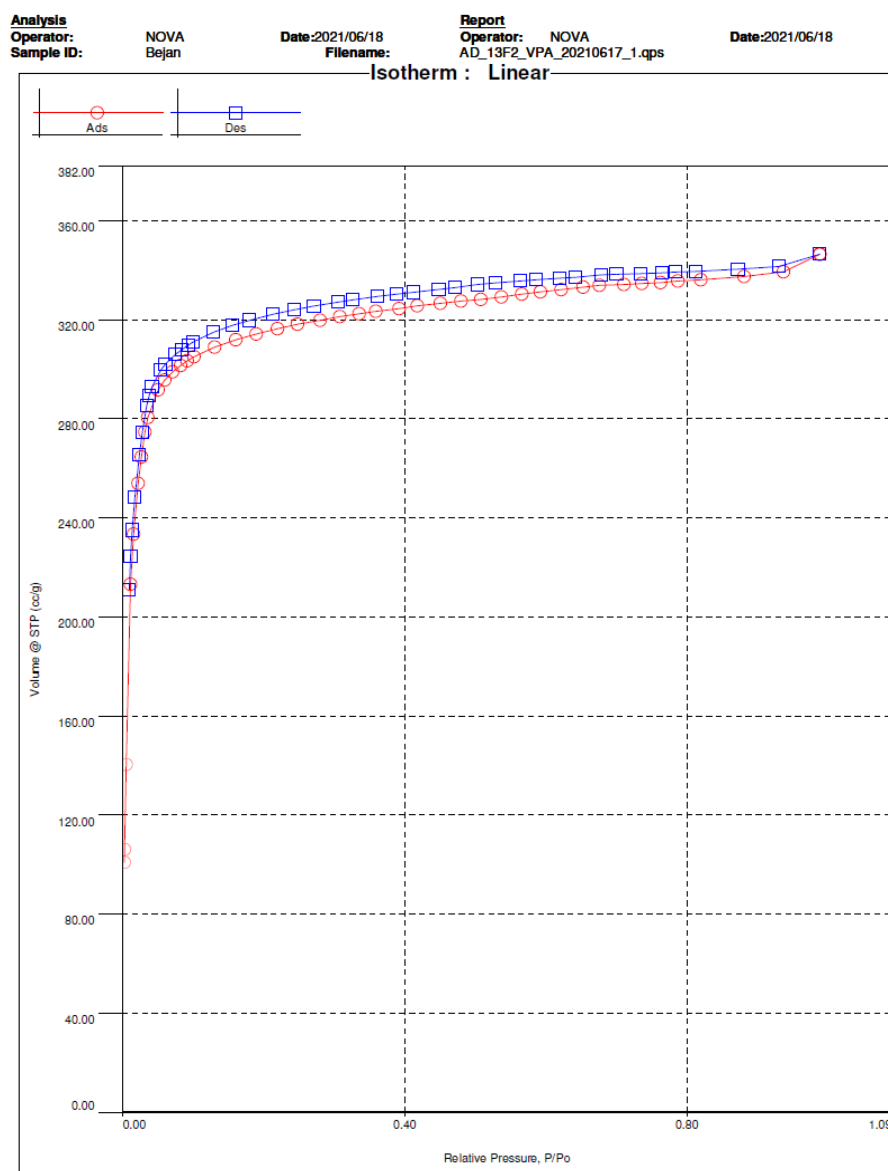


**Figure 9.** Nitrogen adsorption (red) and desorption (blue) isotherm of Zr-F2 MOF after thermal activation;  $S_{\text{BET}} = 1304 \text{ m}^2/\text{g}$ . Total pore volume =  $5.249\text{e-}01 \text{ cc/g}$  at  $P/P_o = 0.93695$ .

The synthesis, characterization and properties evaluation of MOFs composed of the aromatic fluorinated ligands and zinc have also been accomplished.

In the synthesis experiments various solvents were tested, such as DMF, DEF or dimethylacetamide. Initially no modulator was used and as a consequence, the first tests were deployed at 70 °C. Notable results were obtained from the solvothermal reaction (70 °C, 72 h) using the 2',5'-bis(trifluoromethyl)-[1,1': 4',1''-terphenil]-4,4''-dicarboxylic acid H<sub>2</sub>CF<sub>3</sub> and zinc nitrate in DMF. The identified reaction conditions afforded the isolation of the zinc MOF as crystals which allowed the identification of the structure of the compound (Figure 10). In the case of the two other ligands H<sub>2</sub>F<sub>2</sub> and H<sub>2</sub>F<sub>4</sub>, all synthesis experiments afforded microcrystalline powders.

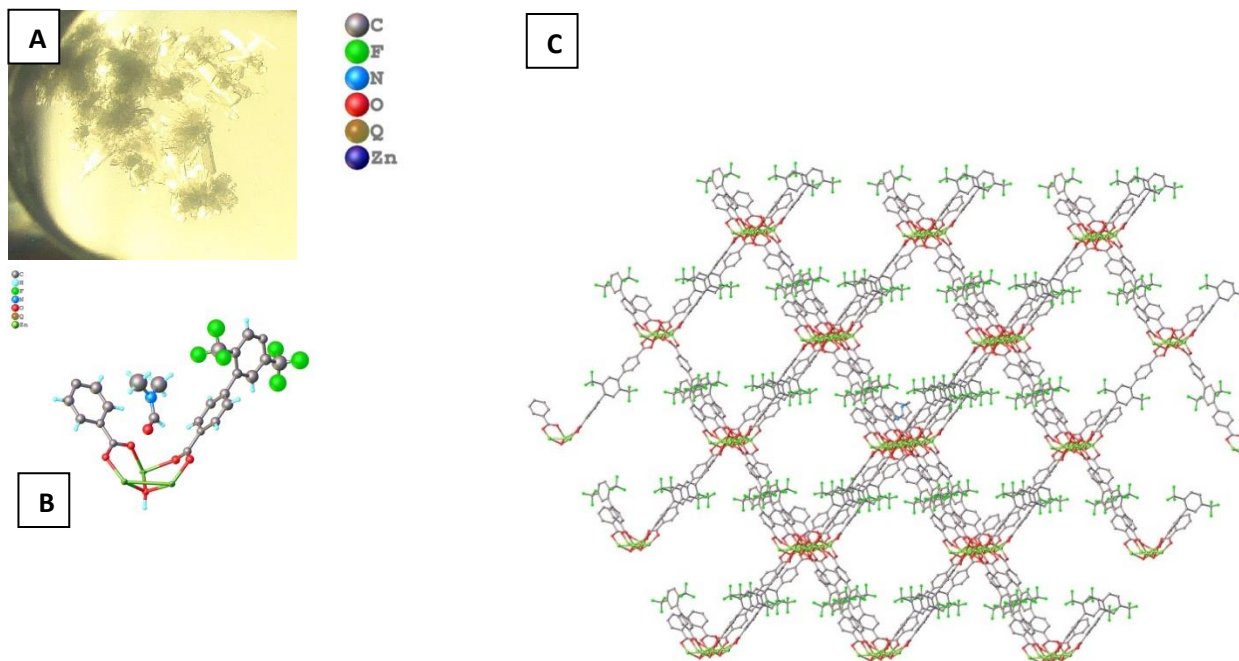


**Figure 10.** Microscope image of the crystals (A) obtained in the synthesis experiment between the 2',5'-bis(trifluoromethyl)-[1,1': 4',1''-terphenil]-4,4''-dicarboxylic acid H<sub>2</sub>CF<sub>3</sub>, zinc nitrate in DMF, the asymmetric unit (B) and the 3D structure of the MOF Zn-CF<sub>3</sub>.

The phase purity of the Zn-CF<sub>3</sub> MOF and the iso-structural relationship with the analogues Zn-F<sub>2</sub> and Zn-F<sub>4</sub> (obtained as microcrystalline powders) were established by pXRD (Figure 11). The small differences observed between the calculated and measured diffractograms for the Zn-CF<sub>3</sub> sample were attributed to the fact that the DMF solvent molecules were not “squeezed” from the single crystal structure.

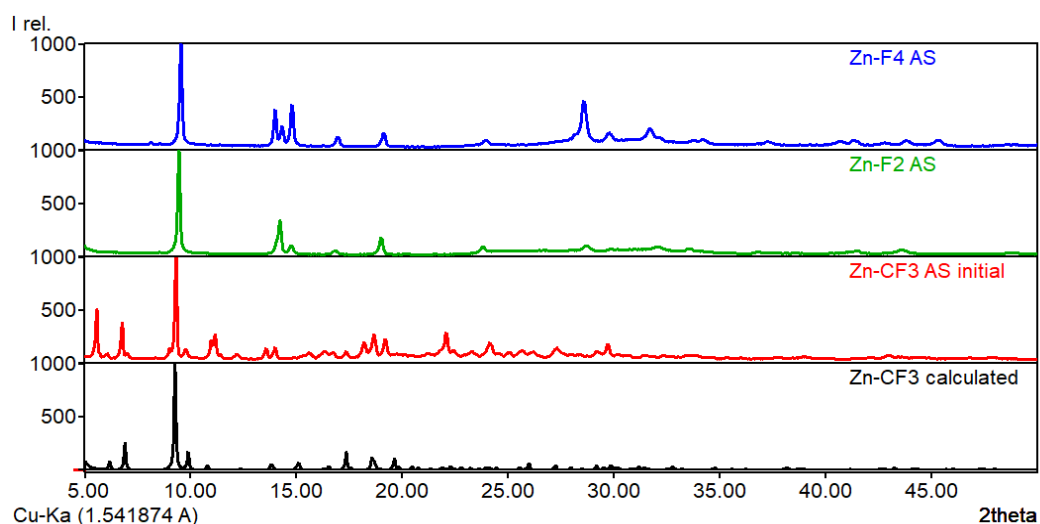


**Figure 11.** The calculated (black) diffractogram of the Zn-CF<sub>3</sub> MOF vs the measured one (red) and that of the analogues Zn-F<sub>2</sub> (green) and Zn-F<sub>4</sub> (blue).

The influence of temperature on the reaction speed and phase purity was also tested. The results showed that conducting the reaction at 90 °C does not speed the process considerably, but the reaction product is formed as well defined independent crystals. The reaction protocol deployed at 90 °C was validated in triplicate at the same scale and later was up-scaled (2x and 4x). pXRD was used to confirm that the same product was formed and that the phase purity was optimal (Figure 12). The purification of the zinc MOFs was accomplished by repeated washing with DMF, centrifugation and removal of the supernatant, followed by a rapid washing with methanol and drying in an oven at 80 °C. The reaction yield in all the repeated experiments at the same scale or up-scaled was between 50-60%.

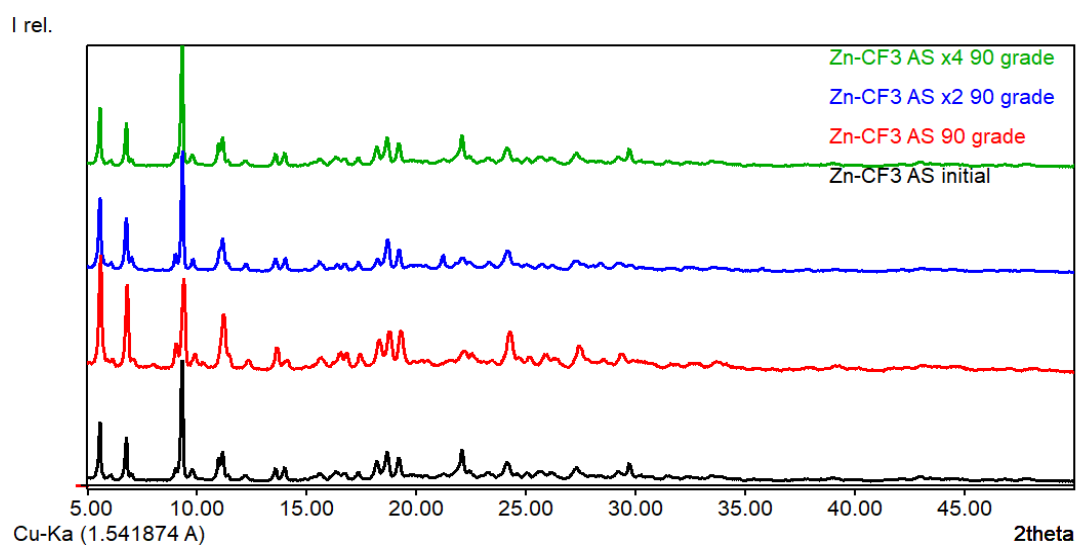


**Figure 12.** pXRD diffractograms of the initial as-synthesized MOF Zn-CF<sub>3</sub> (black), in comparison with the product synthesized at 90 °C at the same scale (red), up-scaled 2x (blue) and 4x (green).

Evaluation of the thermal stability by TGA (Figure 13) indicated that the 3D network begins the decomposition process after 450 °C. Due to its porous nature, the MOF retains a large quantity of solvents in its pores as evidenced by a 25 % mass loss in the 50-225 °C interval.

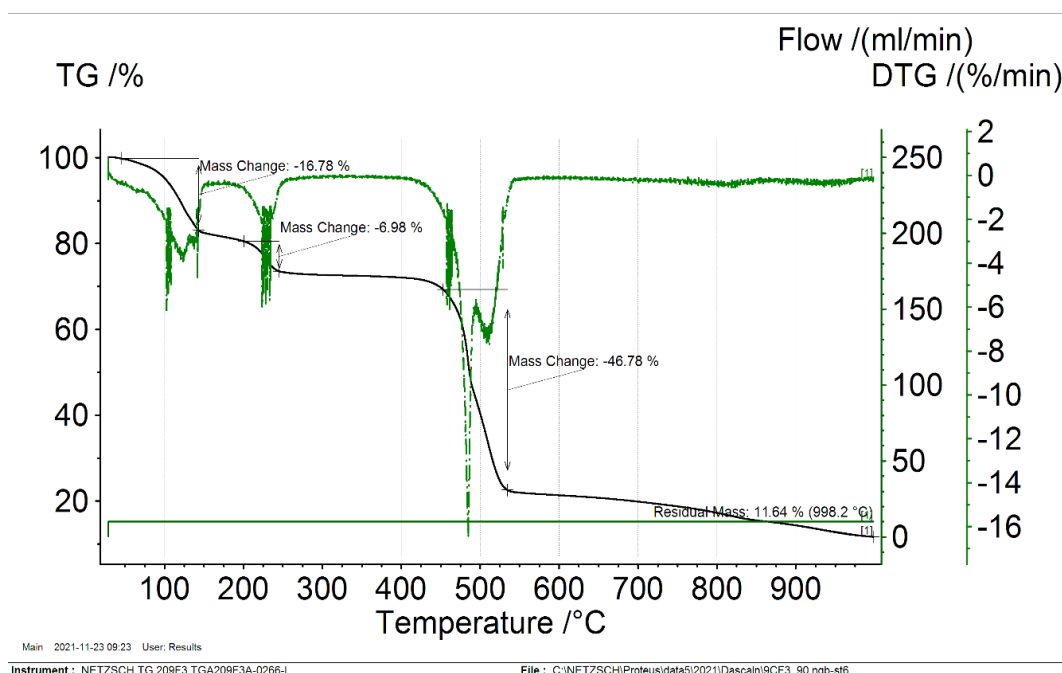


**Figure 13.** Zn-CF3 MOF TGA-DTG curve.

The direct thermal activation of the zinc MOFs at 120 °C for 16 h proved to be insufficient, as evidenced by the small  $S_{\text{BET}}$  values obtained from the nitrogen sorption measurements (below  $50\text{m}^2/\text{g}$ ). In this context, with the help of the Mentor (**Objective 5**), the activation of the metal-organic frameworks by solvent exchange (replacing the adsorbed/coordinated high boiling points solvents with lower boiling point analogues) was accomplished. Two solvent exchange methods were evaluated, whilst screening for structural modifications by pXRD. (*Chem. Soc. Rev.*, 2020, 49, 2751-2798.).

The first approach was made by replacing the retained and coordinated DMF molecules with ethanol. To this purpose, the Zn-CF3 MOF was lightly dispersed in absolute ethanol (25 mL). After approx. 6 h, the dispersion was centrifuged, the supernatant discarded and fresh ethanol was added. The process was repeated four more times. In the final step the product was dried in an oven for 18 h at 80 °C. The sample was then activated at 150 °C for 18 h under vacuum ( $1.8 \times 10^{-2}$  mbar). Nitrogen sorption measurements revealed a slight increase in the BET surface value ( $141\text{m}^2/\text{g}$ ). (**Objective 3**)

After each process step (AS-as synthesized, SE-solvent exchange and activated-thermal activation under vacuum) the samples were evaluated by pXRD. The diffractograms revealed that a partial degradation of the network does take place during the solvent exchange process and after the thermal activation as evidenced by the broadening of the diffraction peaks due to the decrease in crystallite size.

In this context, a different solvent exchange process was tested, using methylene chloride  $\text{CH}_2\text{Cl}_2$ . To this purpose, the Zn-CF3 MOF was lightly dispersed in  $\text{CH}_2\text{Cl}_2$  (25 mL). After approx. 6 h, the dispersion was centrifuged, the supernatant discarded and fresh  $\text{CH}_2\text{Cl}_2$  was

added. The process was repeated four more times. In the final step the product was dried in an oven for 18 h at 80 °C. The sample was then activated at 150 °C for 18 h under vacuum ( $1.8 \times 10^{-2}$  mbar). Nitrogen sorption measurements revealed an improvement in the  $S_{\text{BET}}$  value up to 464  $\text{m}^2/\text{g}$  (Figure 14). (**Objective 3**)

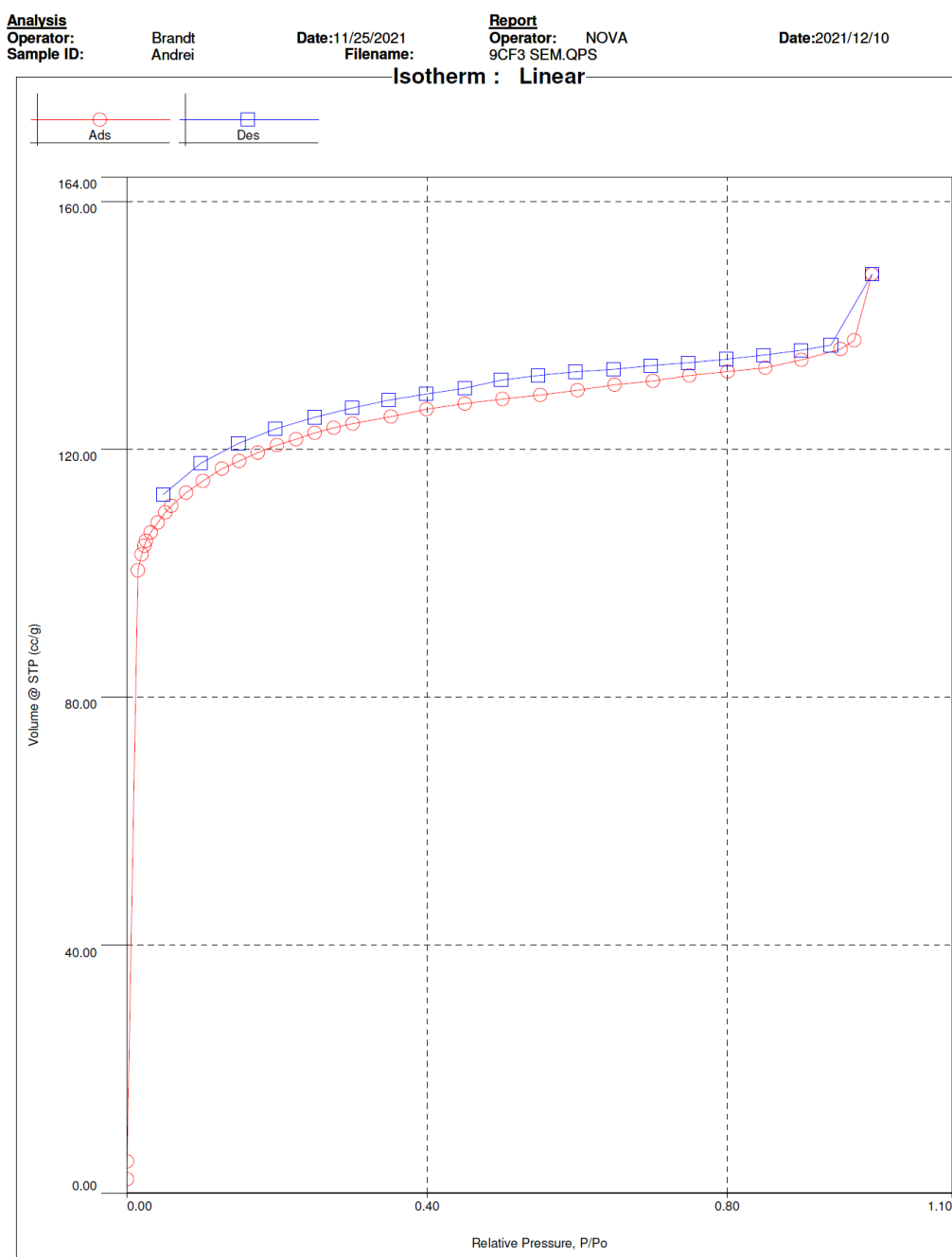


**Figure 14.** Nitrogen adsorption (red) and desorption (blue) isotherm of Zn-CF<sub>3</sub> MOF after SE with CH<sub>2</sub>Cl<sub>2</sub> and thermal activation;  $S_{\text{BET}} = 464 \text{ m}^2/\text{g}$ .

After each process step (AS-as synthesized, SE-solvent exchange and activated-thermal activation under vacuum) the samples were evaluated by pXRD (Figure 15). The diffractograms revealed that a partial degradation of the network does take place during the

solvent exchange process and after the thermal activation as evidenced by the broadening of the diffraction peaks due to the decrease in crystallite size. Although some degradation does occur, it is less pronounced when comparing the diffractograms with those measured after the solvent exchange with ethanol.

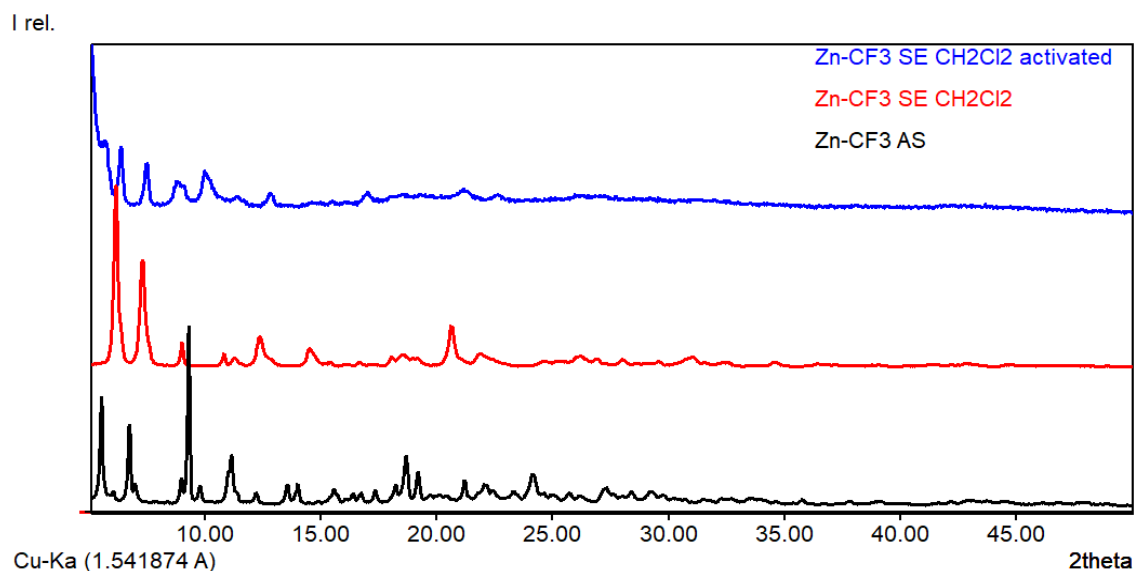


**Figure 15.** The pXRD diffractogram of the as synthesized coordination polymer Zn-CF3 (black) vs that of the product after solvent exchange with CH<sub>2</sub>Cl<sub>2</sub> (red) and that after the thermal activation (blue).

The synthesis of MOFs using the three ligands and aluminum nitrate or chloride has also been accomplished. **(Objective 2)**

DMF was used as the reaction solvent. The reaction temperature and the absence or presence of nitric acid (modulator) were tested. Before heating the reaction vials to the desired temperature, the reaction mixtures were homogenized in an ultrasound bath for 15 minutes. Regardless of the reaction conditions used, all the isolated compounds were microcrystalline powders; single crystal X ray diffraction could not be used to identify the structure of the compounds. Deploying the synthesis reaction in the presence of nitric acid had not considerably influenced the crystallite size of the compounds (Figure 16).



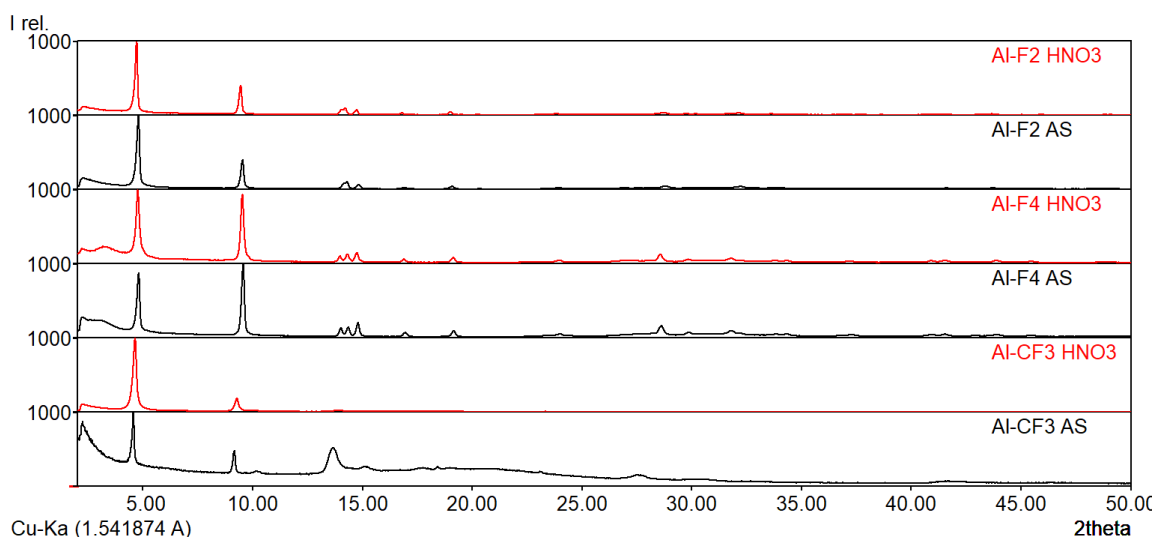


**Figure 16.** pXRD diffractograms of the coordination polymers Al-CF<sub>3</sub>, Al-F<sub>4</sub> and Al-F<sub>2</sub> prepared without nitric acid (black) in comparison with the diffractograms corresponding to the same MOFs prepared in the presence of nitric acid (red).

The purification of the aluminum MOFs was accomplished by repeated washing with DMF, centrifugation and removal of the supernatant, followed by a rapid washing with methanol and drying in an oven at 80 °C. After drying the thermal stability of the Al MOFs was evaluated, all three displaying a similar behavior when heated (Figure 17)-**Objective 3**.

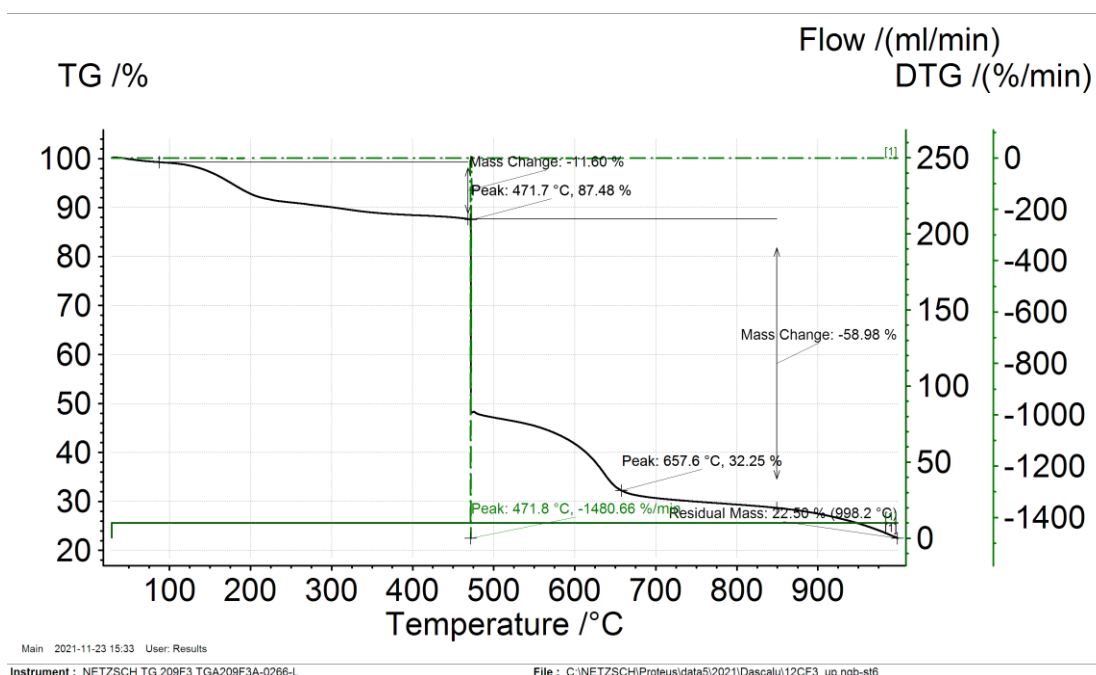


**Figure 17.** Al-CF<sub>3</sub> MOF TGA-DTG curve.

In the 50-470 °C an 11.6 % mass loss was observed due to the removal of the adsorbed and coordinated solvents. The actual thermal degradation of the network begins after 470 °C, which is an adequate thermal resistance threshold for a large number of MOF applications.

In terms of gas storage capacity notable results were obtained in the case of the Al-CF3 MOF that was synthesized in the absence of an acid modulator (90 °C, 72 h). The product was purified by repeated washing with DMF, after which it was subjected to solvent exchange with methylene chloride. In the last step, the Al MOF was activated under vacuum at 200 °C for 4 h. The nitrogen adsorption and desorption isotherms are presented in Figure 18. The determined BET surface was **1693 m<sup>2</sup>/g**. The BET surface values of the iso-structural MOFs Al-F2 and Al-F4 prepared and processed in similar conditions was 439 m<sup>2</sup>/g and 452 m<sup>2</sup>/g respectively.

The products obtained in the presence of nitric acid showed a large decrease in the BET surface values in the case of Al-CF3 (768 m<sup>2</sup>/g) and Al-F2 (279 m<sup>2</sup>/g), while for Al-F4 a slight increase was observed (669 m<sup>2</sup>/g). This phenomena was observed and recently reported in the literature (*Z. Anorg.Allg.Chem.* 2022, 648, e2021003). Even though in accordance with the pXRD data the Al MOF with each aromatic ligand are iso-structural the difference in BET surface values greatly differ. The difference can be attributed to the lower solubility of the H2F2 and H2F4 ligands in comparison with that of the H2CF3 analogue. The solubility difference was observed in the ligands purification step, when for the recrystallization of approx. the same quantity of ligand, a 10 times greater quantity of DMF was needed for the complete dissolution of the H2F2 and H2F4 compounds. In this context, it is very likely that the pores of the Al-F2 and Al-F4 networks, could be blocked by unreacted ligand molecules or molecule clusters.

**Analysis**

Operator:  
Sample ID:

Brandt  
Andrei

Date:11/25/2021  
Filename:

**Report**

Operator: NOVA  
12CF3 SEM.QPS

Date:2021/12/10

**Isotherm : Linear**

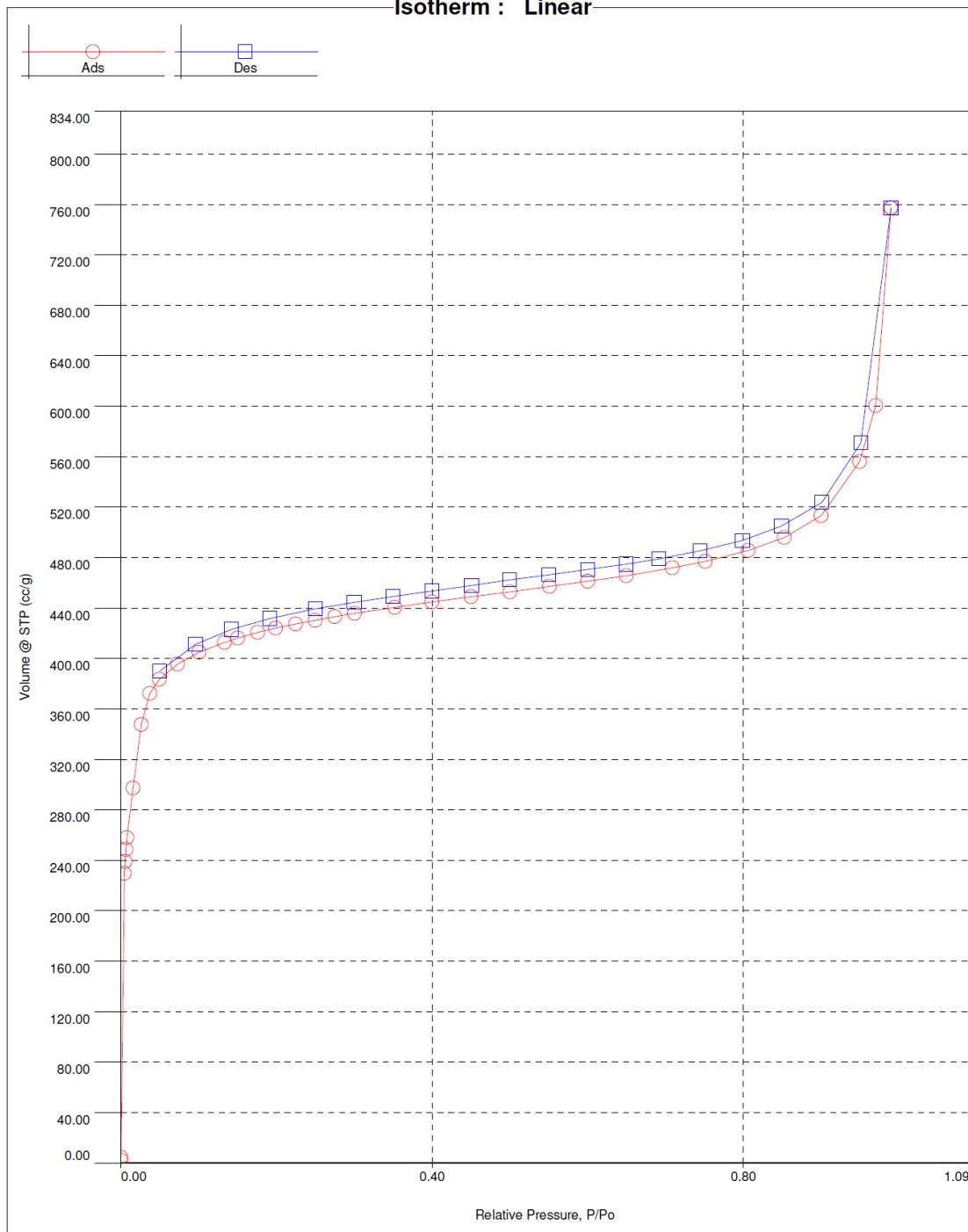


**Figure 18.** I Nitrogen adsorption (red) and desorption (blue) isotherm of Al-CF<sub>3</sub> MOF after SE with CH<sub>2</sub>Cl<sub>2</sub> and thermal activation;  $S_{BET} = 1692.97 \text{ m}^2/\text{g}$ ; total pore volume =  $9.288\text{e-}01 \text{ cc/g}$  at  $P/P_o = 0.96983$ .

In the framework of the project, a research stay (1.11.2021-1.12.2022) was performed abroad at the Institute for Inorganic Chemistry and Structural Chemistry Heinrich-Heine-University Düsseldorf, Germany, under the supervision of the Mentor Prof. Dr. Christoph Janiak. **(Objective 5)**

A part of the results were disseminated by means of an oral presentation entitled „METAL-ORGANIC FRAMEWORKS BASED ON A FUNCTIONALIZED TERPHENYLDICARBOXYLIC ACID FOR GAS AND WATER SORPTION” at SESIUNEA DE COMUNICARI STIINTIFICE A TINERILOR CERCETATORI, POARTA DESCHISA SPRE VIITOR, 19 November 2020, Iasi, Romania. **(Objective 4)**

In addition part of the obtained results have been disseminated at “Progress in Organic and Macromolecular Compounds 28th Edition” Iasi, Romania, 7 – 9 October 2021 with a poster presentation entitled „TOWARDS ROBUST METAL-ORGANIC FRAMEWORKS BASED ON FLUORINATED LINKERS FOR GAS STORAGE” (<https://icmpp.ro/macroiiasi2021/files/proceedings-POMC.pdf>). During this conference, the poster presentation was awarded the **Best Poster Communication** award (<https://icmpp.ro/macroiiasi2021/>). **(Objective 4)**

The results obtained from the successful implementation of the project activities were published **(Objective 4)** in two papers in Web of Science indexed journals, one of which was open access and a patent request:

1. I.-A. Dascalu, D.-L. Isac, S. Shova, M. Balan-Porcarasu, N.-L. Marangoci, M. Pinteala, C. Janiak, Structural characterization and computational investigations of three fluorine-containing ligands with a terphenyl core, *Journal of Molecular Structure*, 1266, **2022**, 133474.

2. Bejan, D.; Dascalu, I. A.; Shova, S.; Trandabat, A. F.; Bahrin, L. G. Mesitylene Tribenzoic Acid as a Linker for Novel Zn/Cd Metal-Organic Frameworks, *Materials*, **2022**, 15, 4247.

3. Cerere brevet de inventie: RETEA METAL-ORGANICA CU LIGAND TRITOPIC SI PROCEDEU DE OBTINERE, Bahrin L., Bejan D., Dascalu I.-A., Sova S., Marangoci N.-L., Ardeleanu T.-S., Registratura OSIM nr. A/00431/21.07.2022.

A third manuscript is underway and will be sent for publication by the end of the year 2022.

### The impact of the obtained results

The successful implementation of this project resulted in the identification of an experimentally validated approach for the synthesis, characterization and molecular modeling of the three proposed ligands. In addition the identification of the X-ray molecular structure of all three aromatic dicarboxylic acids allowed the calculation of the Hirschfield surface analysis, which identifies the supramolecular packing and atom proximities in the crystalline solid. The theoretical investigations are valuable resources useful in identifying the structural particularities encountered in the structure of the MOFs prepared with these ligands and in explaining the gas sorption or separation behavior of the coordination polymers.

In addition, using the three ligands, robust zirconium, zinc and aluminum MOF have been prepared with **excellent thermal stability (higher than 450 °C)**. The BET surface area of the MOF especially those with tetravalent **Zr-F2** or trivalent metals **Al-CF3** of **1300** and **1690 m<sup>2</sup>/g** respectively, alongside the chemical and thermal resistance imparted by the robust metal-ligand bonds, recommends these MOFs as viable candidates in gas sorption.

Director Proiect,

Dr. Ioan-Andrei Dascalu



Further information concerning this project can be found at:

<https://icmpp.ro/projects/11/about.php?id=19>